Stability Studies in Pipe Flows Using Water and Dilute Polymer Solutions

NEIL S. BERMAN and EUGENE E. COOPER

School of Engineering
Arizona State University, Tempe, Arizona 85281

The response of water and 20 ppm. solutions of Separan AP-30 and Polyox WSR 301 to the periodic motion of a thin sleeve was measured using a laser Doppler velocimeter. The sleeve was moved in an axial direction by an external coupling at frequencies from ¼ to 1.0 Hz and at amplitudes of ½ to 2 in. The flow field downstream of the disturbance was found to consist of three regions: 1. a near field with a separation wake from the sleeve moving toward the pipe centerline; 2. an intermediate field in which alternate laminar and turbulent slugs passed a point; and 3. a far field with decaying turbulent flow. Differences in the behavior of water flows and polymer flows appeared in each region. In the near field, wakes spread faster in water flows. In the intermediate field, the laminar slugs disappeared into turbulence more rapidly in water flows. And in the far field, the turbulence was not as developed in the polymer flows.

Detailed statistical evaluations were made on the signals in each region for a Reynolds number of 2000. The response of the dilute polymer solutions appeared to be governed by the initial interaction with the sleeve. Fewer high frequencies were generated than in the pure solvent so the periodic disturbance persisted downstream. In pure water the eddies from the separation wake interacted strongly with the periodic disturbance leading to rapid decay of the periodic portion. Shear rates were not high enough to attribute the dilute polymer differences to viscoelastic effects.

Current interest in drag reduction has led to many studies of the behavior of dilute polymer solutions in pipe flows. One unusual property observed in laminar flow at Reynolds numbers below 200 is a decreased entry length compared to the pure solvent (*2*). However, the opposite has been found for turbulent flow (*12, 26*). The laminar flow behavior was attributed to the non-Newtonian properties of the dilute polymer solutions at low shear rates, but viscoelastic properties are suspected to influence the flow at high shear rates. In some cases the dilute polymer solutions also have a delayed transition to turbulence. That is, turbulent flow is obtained only at Reynolds numbers above the limit for the pure solvent. Recent studies by Chung (*10*) and Poreh et al. (*24*) show delayed transitions in some fresh solutions such as polyethylene oxide in water, no delay in degraded solutions, and a reduction of the transition Reynolds number in polyisobutylene solution. The entry and transition flows are related to the growth and decay of disturbances in laminar flow, (stability), as well as to the propagation and decay of turbulence, (transition). This study was undertaken to see if experimental differences in the behavior of an artificially introduced oscillation in water and dilute polymer solutions could be related to stability or transition.

Some measurements are available on transition flow of dilute polymer solutions, for example, Goldstein et al. (*19*), White and McEligot (*28*), Castro and Squire (*8*), Chung (*10*) and Poreh et al. (*24*). These studies also show unsteady behavior at various laminar and transition Reynolds numbers even when pure water flow is laminar. Experimental measurements of the behavior of disturbances in pipe flows of liquids are rare although there have been many theoretical studies. The stability of fully-developed flows subjected to small disturbances has been studied experimentally by Leite (*21*) and by Bhat (*5*). In Leite's experiments, Poiseuille air flow in a 1¼-in. diam. tube was subjected to periodic axial motion of an axisymmetric sleeve. Radial traverses of the velocity field showed, however, that the small induced velocity fluctuations were not axisymmetric. The nonaxisymmetric disturbances decayed faster than the axisymmetric portions, even at a Reynolds number of 13,000. Bhat used a flat spring disturbance generator which was caused to vibrate by an alternating magnetic field imposed outside his 1-in. diam. tube. The resulting disturbance was small, nonaxisymmetric, and azimuthally periodic. Bhat found that the disturbances could become unstable, and the appearance of instabilities depended upon the Reynolds number and the vibration frequency. Bhat continued his experimental investigation with azimuthal disturbances into the entry region, 10

diameters and 15 diameters from the inlet. At 10 diameters, he found that the mere presence of the disturbance generator, even when not vibrating, caused transition at Reynolds numbers over 3,000. At lower Reynolds numbers, the flow was stable to the presence of the stationary generator, but vibrating it caused a transition. The history of the problem for both small amplitude and finite amplitude disturbances has been reviewed by George (*17*) for Newtonian fluids. The problem in general has not been solved for either the Newtonian or the non-Newtonian fluid. Viscoelastic fluids apparently can be more or less stable than a Newtonian fluid as demonstrated by Ginn and Denn (*18*) and Denn and Roisman (*11*). Another interesting study by Patten and Schechter (*23*) considers the effect of slightly elastic fluids on the stability of laminar flow to small disturbances. However, it is difficult to relate the theoretical studies on small disturbances or the solutions for specific large disturbances to a real experimental situation. The work reported here consisted of examining visually and point by point with a laser Doppler velocimeter the response of water and dilute polymer solutions to a large disturbance. These measurements are believed to be the first studies of this form of disturbance ever reported for dilute polymer solutions.

EXPERIMENTAL APPARATUS

Flow velocities in the axial direction at a point in the tube were measured with a laser Doppler velocimeter previously described (*4*). The laser Doppler velocimeter provides a method of measurement which does not disturb the flow, and fluctuations at a point in the fluid can be measured. Using the methods outlined by Edwards et al. (*13*), the measurements in this work correspond to a scattering volume 100-300 microns long by 10-30 microns in diameter, approximately a cylinder with the long axis along a diameter of the tube.

For unsteady flow measurements, a continuous tracking of the frequency is necessary or an exact knowledge of the frequency broadening. The system is too complex to determine the broadening, but if everything is constant except the time variations of the velocity, the heterodyne signal can be tracked using the system described by Hanson et al. (*20*). In this method the signal is amplified using a broadband amplifier, then a Hewlett-Packard Model 3410A microvoltmeter is used as a tracking amplifier to provide a 4-v. sq. wave input to a frequency meter. A plot of the variation of an "average" instantaneous signal with time can then be obtained from the frequency meter as shown in Figure 1. This tracking system was calibrated with the center line velocity of a known laminar flow and checked by rotating a ground glass disk at a constant velocity. Fluctuations measured using this method were less than 1% for laminar flow at the center line and approximately 4% for fully developed turbulence.

The flow system was the same as used by Hanson et al. and Burke and Berman (*7*) except for the return pump on the constant head system for the dilute polymer solutions. For the dilute polymer studies, a roller pump or a piston pump with a 2-in. cylinder and 4-in. stroke was used to return the liquid to the upper constant head tank. A test section of three 4-ft. long pieces of 0.543-in. inside diam. glass tube joined by nylon fittings was used in addition to the 1-in. diam. glass pipe used by Hanson. The flow system and tube mountings were the same as described by Burke and Berman. With capillaries on the downstream end of the system ahead of the lower constant head tank, constant flow could be maintained for Reynolds numbers up to 4,000.

Disturbances of the flow in the test section were generated at various distances upstream of the scattering volume or measurement point. The disturbance generator was a cylindrical brass sleeve with an iron insert. The sleeve was the same as Hanson's for the 1-in. pipe and 0.523-in. outside diam., 0.445-in. inside diam. and 1 in. long for the smaller tube. When the sleeve was inside the glass tube, it could be moved by a permanent magnet attached to a "scotch" yoke outside the tube. The frequency could be varied from zero to two Hz and the amplitude from ½ in. to 2 in. The total sleeve travel was twice the amplitude.

The fluids used were water, 20 ppm. Separan AP-30, and 20 ppm. Polyox WSR 301. The dilute polymer solutions were mixed in concentrated form and then diluted to the final concentration. The properties of the fluids were checked by repeating the experiments. In all cases newly mixed solutions behaved the same, and steady flow measurements at Reynolds numbers below 500 were repeatable regardless of the condition of the fluid. Degraded solutions usually had similar unsteady behavior to the fresh solutions in laminar flow but differed greatly in turbulent flow or transition flow.

To improve light scattering intensity, 0.5 micron polystyrene spheres were added to the fluids in a concentration of one part per 50,000 parts of fluid. Electron photomicrographs of the solutions after evaporation of water showed that the polymers did not coil around the spheres but were elongated and attached to the spheres only at the ends, if at all. Similar results were obtained by spraying the solutions onto the electron microscope grids or evaporation from drops. The polymers were made visible after shadowing with uranium.

Flow Visualization

In order to clearly interpret the laser Doppler results, a flow visualization technique was used to study gross flow characteristics. Aluminum flakes were added to water and the flows through the flow tube were set equal to those used in the laser Doppler work. The visualization setup revealed that the nylon fittings joining the glass tubes did not affect the flow. No eddies were created by the stationary disturbance. However, turbulent slugs could be created in the entrance region of the tube and would propagate along the tube when the Reynolds number was sufficiently high.

When laminar flow entered the moving sleeve, the flow leaving was also laminar if the sleeve moved forward. But when the sleeve moved against the flow, distinct eddies were created. The result was an alternating region of laminar and eddy flow immediately downstream of the sleeve. At low Reynolds numbers the alternate regions continued separately downstream and the eddy flow rapidly decayed. At higher Reynolds numbers, the eddy regions expanded into the laminar region within one wavelength distance downstream. Here wavelength is approximately the flow velocity divided by the sleeve oscillation rate. The resulting flow looked like turbulent flow which could be generated in the entrance region except for one characteristic. The eddy flow after the sleeve did not propagate downstream. The eddies migrated to the center, elongated and

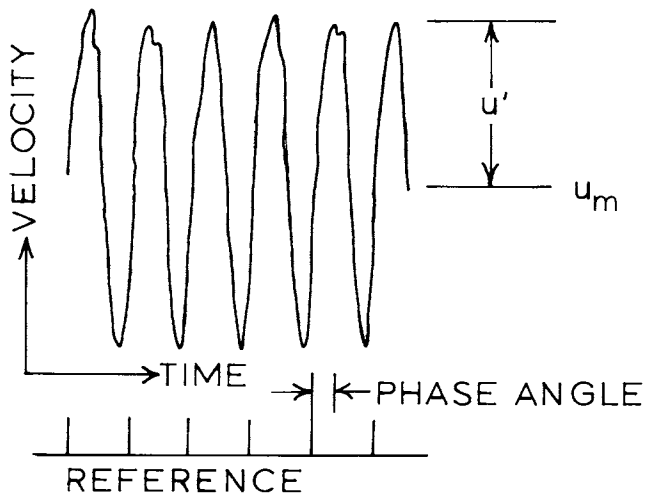

Fig. 1. Typical data point.

finally died out all in a well defined part of the tube.

The eddies shed by the backward moving sleeve were due to flow separation at the wall. When the sleeve moved backwards, the fluid at the wall was moved counter to the mainstream flow direction, a condition of flow separation. The decay of the disturbance indicated that the flow was stable to both the eddy creation and the overall sleeve motion. This decay was observed at all Reynolds numbers until the pipe flow in the tube became turbulent upstream of the disturbance and throughout the entire pipe.

LASER DOPPLER STUDIES

The disturbance behavior observed in the flow visualization studies was also distinguishable in the laser Doppler point velocity measurements and quantitative values can be attached to the observations. From the determinations of fluctuation amplitude, mean velocity, and phase angle at the different axial and radial points, plots can be made showing the average disturbance decay. These plots do not show the variations in fluctuation frequency or the distribution of energy among different frequencies. Therefore, the breakup into turbulent eddies shows up as a lowered fluctuation amplitude and a lowered mean velocity. Typical plots of fluctuation amplitude and mean velocity versus the radial coordinate were given by Hanson et al. (*20*) and Berman and Cooper (*3*). At Reynolds numbers below 1,000, the maximum in the amplitude curve does not occur at the centerline and the velocity profile is flattened after the disturbance. The phase angle behaves in a similar manner to that of Leite (*21*) and remains constant near the center of the tube and increases nearer the wall. Berman and Cooper also show several plots of the axial decay of amplitude and mean velocity. The decay of the disturbance is slower than that of Leite and indicates that the distortion of the velocity profile has an influence. Three different types of plots are obtained as shown schematically in Figure 2. Curve (a) shows decay of the fundamental disturbance while the other two curves indicate the interaction of the fundamental disturbance with the eddies that were observed after one wavelength downstream (b), and within the first wavelength (c). The behavior of both water and the dilute polymer solution depends upon the Reynolds number, pipe diameter, and the frequency and amplitude of the disturbance. Increasing Reynolds number, frequency or amplitude will move a response from type (a) to (b) and then to (c). The polymer solutions lagged behind the water response to such changes. Since the polymer differences seemed to be mostly related to this lagged response, detailed analyses are discussed in this work at a condition where the curves for both water and dilute polymer solutions are type (b). Frequencies of 0.25 to 1.0 Hz, total sleeve travels of 1 in. and 2 in., and Reynolds numbers of 1,000 and 2,000 are included. Although velocities were measured at various radial positions, the centerline values are representative and are given here. It was not possible to make measurements closer than 300 microns from the wall using the scattering angle selected for the centerline work and using the electronics available. The disturbance generator was limited to two Hz. At high frequencies it would be impossible to move a sleeve with the large amplitudes that were used. The work of Fox, Lessen and Bhat (*15*) showed that the low end of frequency dependence of the neutral stability curve was between 0.2 and 1 Hz, and the high end around 30 Hz, at least for their azimuthally periodic disturbance. Using the oscillating sleeve in this study, the only definite instabilities that could be found were complete transitions to turbulence. When this occurred at sufficiently high Reynolds numbers, the flow was turbulent whether or not the sleeve was moving. Higher Reynolds numbers were required for fresh dilute polymer solutions than for water to provide the turbulent situation. However, there are differences in the response of the two types of fluids to the oscillating sleeve which can be observed at Reynolds numbers below the transitional. These differences can be related to the response of dilute polymer solutions to disturbances at an entrance or disturbances created at the wall of a pipe before the onset of turbulence.

Figures 3, 4, and 5 show a typical history of the flow downstream of the disturbance in terms of the probability density function (PDF), autocovariance function, and power spectral density function. The first two were obtained directly from the Hewlett-Packard correlator. The power spectrum was calculated from the autocovariance. The probability density function is a plot of voltage versus probability. The voltage from the frequency meter can be converted to the Doppler frequency shift which is proportional to velocity. Interpretation of the PDF's is consistent with the flow visualization study. Little effect of the sleeve oscillation is seen at 2½ in. downstream. The velocity distribution is characteristic of the laser Doppler instrument for laminar flow with a velocity gradient within the scattering volume. This gradient is greater than for the usual laminar case since the sleeve is a slight constriction in

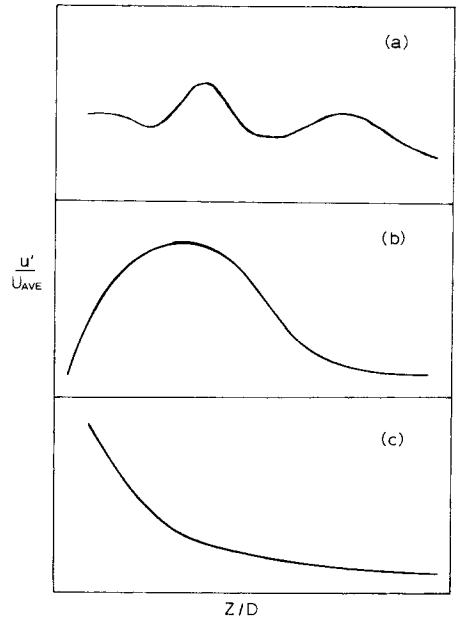

Fig. 2. Three types of growth and decay observed downstream of disturbance.

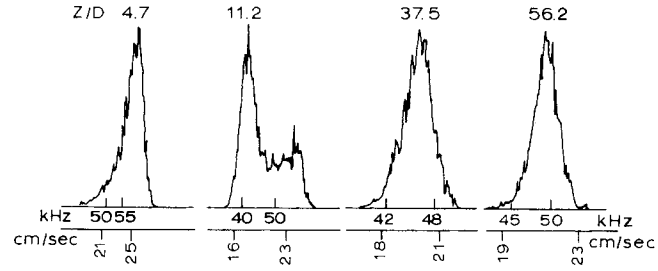

Fig. 3. Probability density function at various downstream points for water at the centerline, ½ Hz, $D = 0.534$ in., 2 in. total amplitude, $N_{Re} = 2000$.

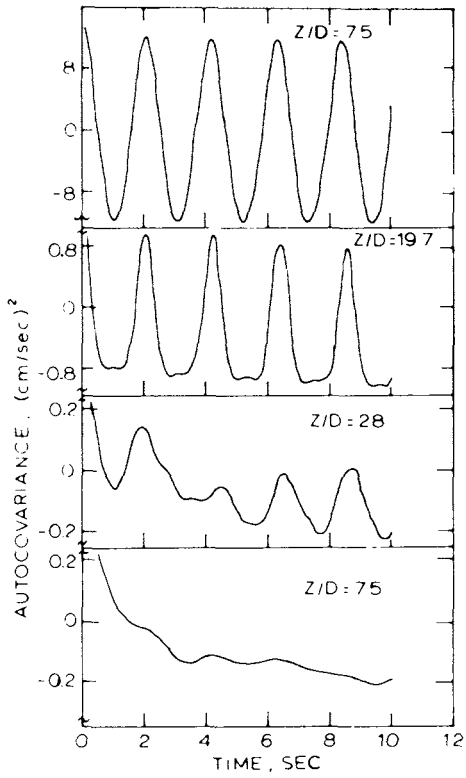

Fig. 4. Autocovariance function at various downstream points for water at the centerline, ½ Hz, $D = 0.534$ in., 2 in. total amplitude, $N_{Re} = 2000$.

the tube and the centerline velocity is higher than twice the mean. At 6 in. downstream, the flow contains both laminar and eddy regions. The total velocity spread is very large and the two separate distributions can be seen [other results at 0.25 Hz by Chang (9) are more pronounced]. The eddy distribution is broader than the laminar part and further downstream the laminar part disappears. The PDF at 20 in. shows only a turbulent situation, but at 30 in. the mean velocity has increased and the variance has decreased indicating a decay of the eddies.

In Figure 5 the changes in the autocovariance $R(\tau)$ are shown for different distances downstream of the oscillating sleeve. At 4 in. downstream, the periodic contribution is dominant and there is little difference between $R(0)$ and the maximum amplitude of the periodic function $R_p(0)$. $R(0)$ is a measure of the square of the total fluctuation on the average. As the distance downstream increases the ratio of $R(0)$ to $R_p(0)$ increases showing the increase of random fluctuations compared to the periodic ones. At 40 in. downstream the autocovariance is almost completely random.

From the Fourier transform of the autocovariance the distribution of frequencies near the original 0.5 Hz can be studied. Figure 5 shows that the disturbance first gains frequencies which are multiples of the fundamental but these multiples disappear more rapidly than the 0.5 Hz fundamental. The 0.5 Hz shows up even at the distance 40 in. from the disturbance but its magnitude is very low. Similar results can be obtained for dilute polymer solutions. Figures 6 and 7 show a comparison of total fluctuation amplitudes at various downstream distances for water and 20 ppm. solutions of Separan AP-30 and Polyox WSR 301. A comparison of these two curves shows that the

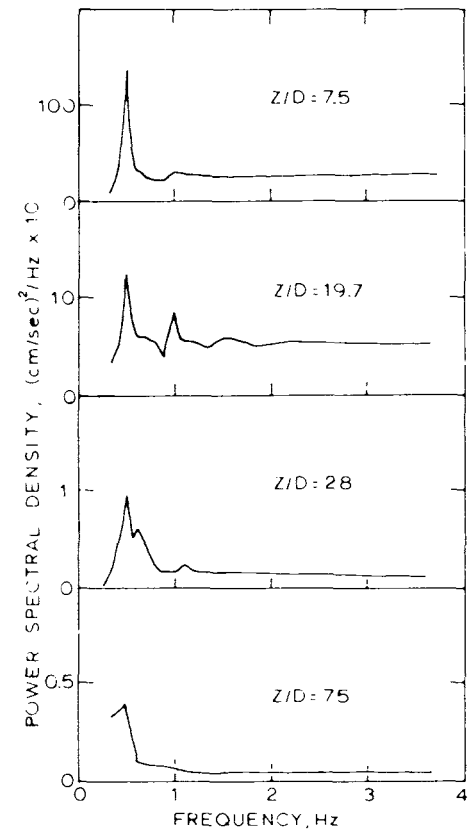

Fig. 5. Power spectral density function at various downstream points for water at the centerline, ½ Hz, $D = 0.534$ in., 2 in. total amplitude, $N_{Re} = 2000$.

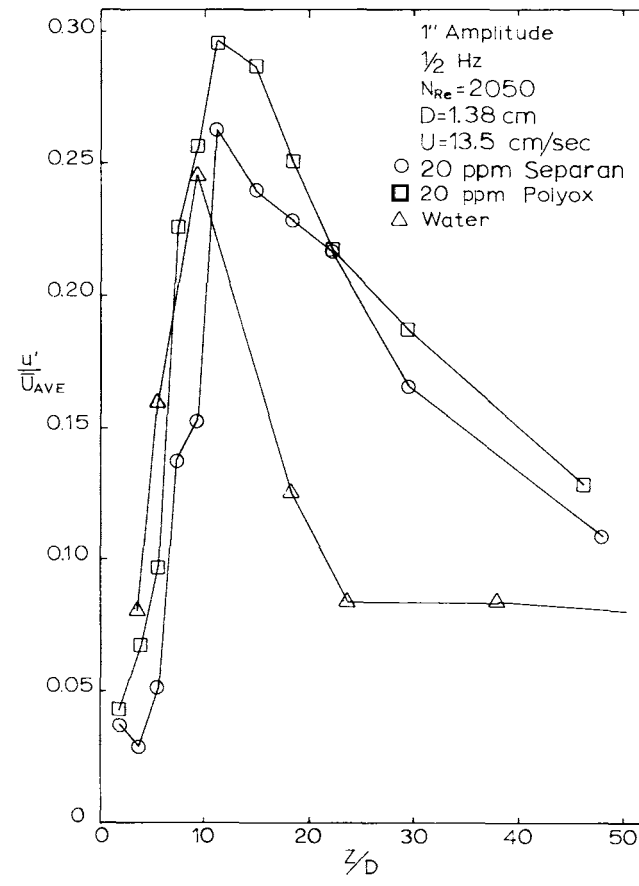

Fig. 6. Fluctuations downstream for ½ Hz, 1 in. total amplitude oscillation.

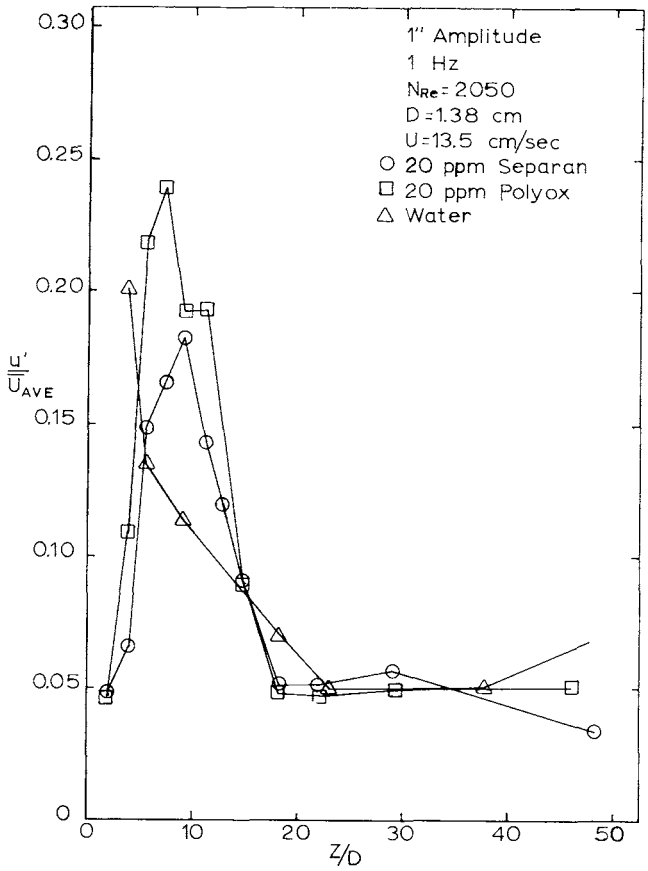

Fig. 7. Fluctuations downstream for 1.0 Hz, 1 in. total amplitude oscillation.

polymer solutions at one Hz act like water at 0.5 Hz for this amplitude. For purposes of comparison, no attempt is made to convert the amplitude to a velocity. Increasing the amplitude is the same as increasing the frequency (3). The fluctuation amplitude shown in Figures 6 and 7 is the same as $R(0)$ of the autocorrelation. Comparison of $R(0)$ and $R_p(0)$ for a polymer solution and water at two different Reynolds numbers is shown in Figures 8 and 9. At $N_{Re} = 1{,}000$ the polymer response is damped but there is not much difference between the location of the maximum values of $R(0)$ and $R_p(0)$ downstream for both. Near transition, however, a considerable portion of the water response is random compared to little for the dilute polymer solution, and the maxima have shifted. Another comparison can be made by plotting the mean velocity at the centerline as in Figure 10. The water drops to a much lower mean velocity at 35 in. from the disturbance. Figures 11 and 12 show two representations of the fluctuations indicating the major difference between the pure water and the dilute polymer solutions is that the frequency distribution is narrower in the polymer solutions.

Throughout all the measurements at the Reynolds number of 2,000 the observations can be summarized as follows:

1. The separation vortices created by the moving sleeve migrated to the centerline faster in water than in the dilute polymer solution. This is similar to differences in wake spreading observed by Barnard and Sellin (*1*). This behavior is termed the near field behavior and includes the distance from the sleeve to the maximum amplitude point at the centerline.

2. The periodic disturbance decayed more rapidly in water than in the dilute polymer solution. This will be called the intermediate field behavior as the decay occurred after the near field.

3. Finally, the flow field consisted of eddies with frequencies much larger than the periodic disturbance. The polymer flows contained less of these eddies and the return to laminar flow was more rapid for the dilute polymer solutions. This area of final decay is called the far field.

DISCUSSION OF RESULTS

The three regions—near, intermediate, and far fields—will be treated separately. A plot of $R(0)$ versus downstream distance Z for constant Reynolds number, diameter, sleeve frequency, and sleeve amplitude has a maximum $R(0)$ at some value of Z, say Z_1. Z_1 is roughly the point at which the eddy-filled wake from the moving sleeve reached the centerline. In the near field the rapidity with which the wakes moved to the center is related to the stress and shear rate at the moving sleeve wall. A higher shear rate at the wall should result in the effects of the stress being felt more quickly away from the wall. A model which can be used to estimate the shear rate can be taken from turbulent boundary layer methods given by Schlichting (*25*).

Consider an observer riding on the sleeve counter to the flow direction. To the observer, it would appear that the fluid particles adjacent to the inside surface of the sleeve

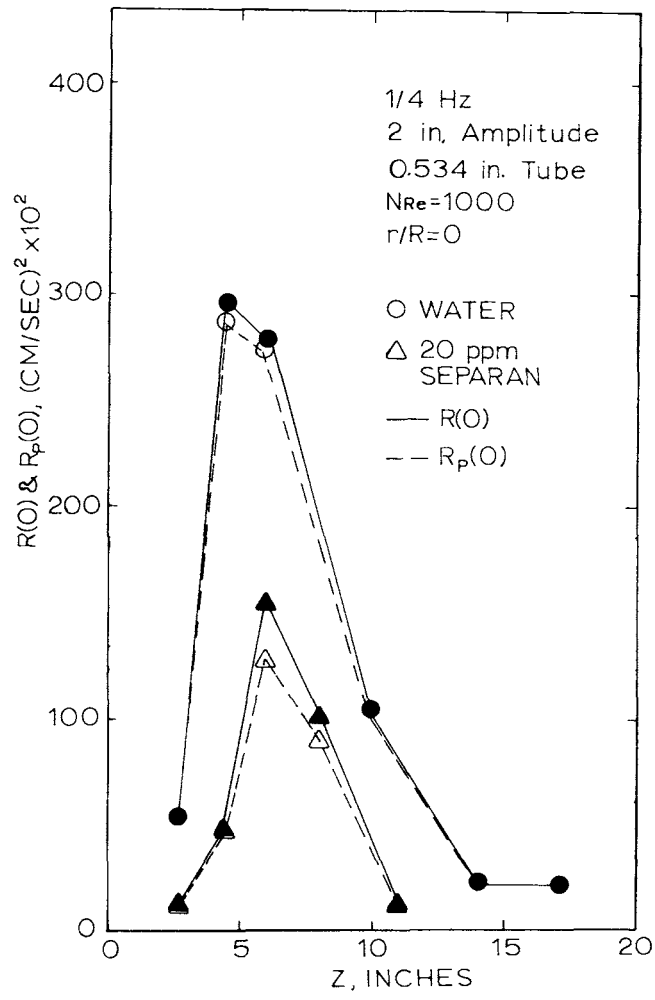

Fig. 8. Fluctuation intensity as a function of distance for water and Separan $N_{Re} = 1000$.

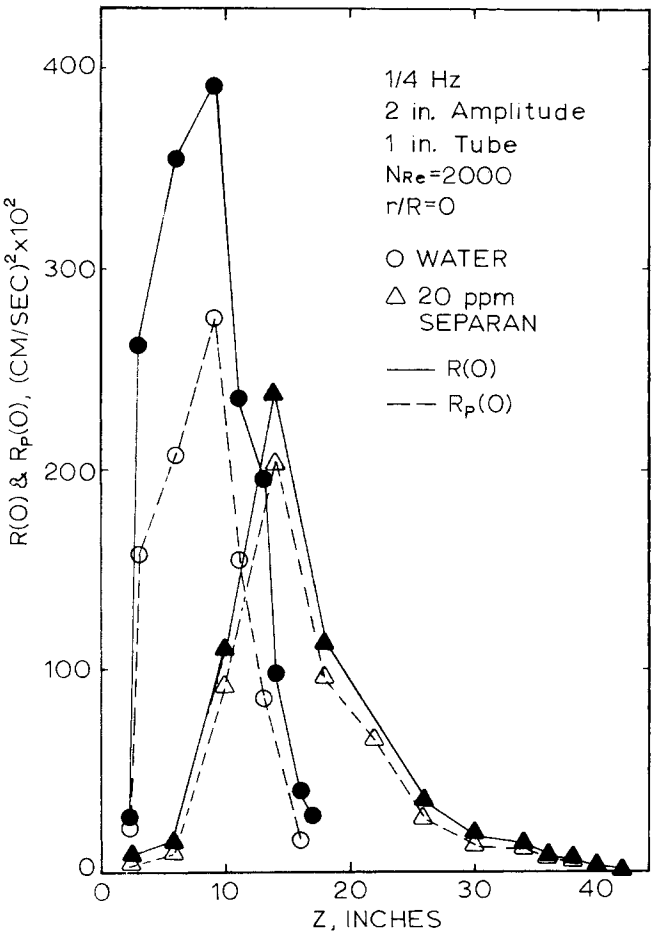

Fig. 9. Fluctuation intensity as a function of distance for water and Separan $N_{Re} = 2000$.

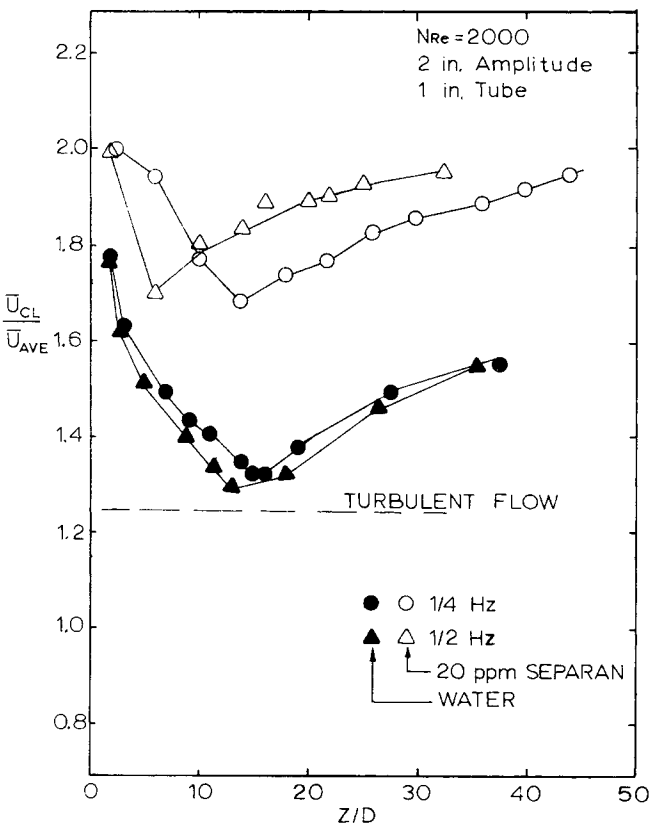

Fig. 10. Mean velocity as a function of distance for water and Separan.

were moving at zero velocity, while those at the centerline were moving with speed (|sleeve velocity| + |flow velocity|). The observer would also see what would appear to him to be a turbulent boundary layer forming at the upstream edge of the sleeve growing inside the sleeve, and continuing growth downstream of the sleeve until the tube centerline was reached by the boundary layer. Naturally, this boundary layer would be growing into the shear layer which the observer would see approaching the sleeve and passing inside it.

The shear stress at the wall beneath a turbulent boundary layer (B.L.) is given by

$$\tau_w = (0.0296)\,[N_{Re}(Z)]^{-1/5}\left[\,2 \times \begin{matrix}\text{dynamic pressure}\\ \text{outside B.L.}\end{matrix}\,\right] \tag{1}$$

where

$$\left[\begin{matrix}\text{dynamic pressure}\\ \text{outside B.L.}\end{matrix}\right] = \frac{1}{2}\rho(|\dot{S}| + |u|)^2$$

$$N_{Re}(Z) = \frac{\rho(|\dot{S}| + |u|)\,(Z - Z_U)}{\mu} \tag{2}$$

The distance of sleeve motion may be described by

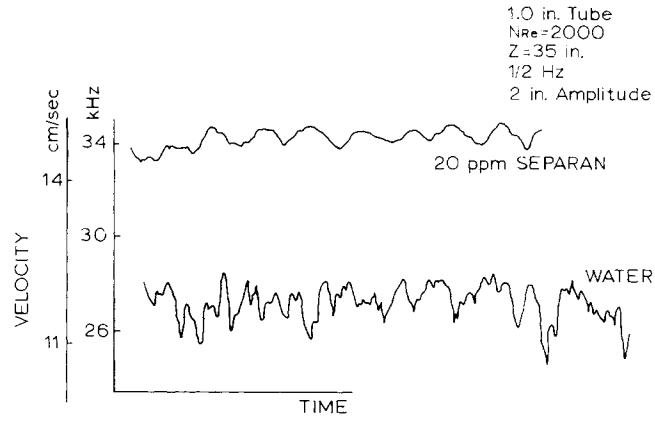

Fig. 11. Comparison of turbulent flow velocity time traces.

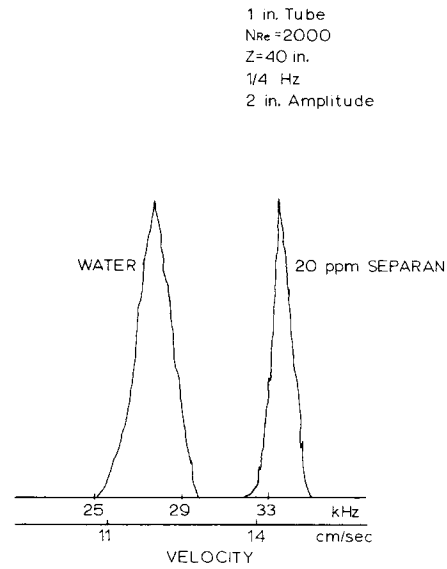

Fig. 12. Comparison of probability density functions for eddy filled regions in water and Separan.

$$S = \frac{B}{2} \sin \omega t \tag{3}$$

Its speed is

$$S = \frac{B}{2} \omega \cos \omega t \tag{4}$$

Here Z is the laboratory coordinate. Z = 0 is the point of furthest downstream movement of the downstream edge of the sleeve. Z_U is the position of the upstream edge of the sleeve with respect to Z = 0, and is the point from which the boundary layer grows. τ_w is related to the shear rate by

$$\tau_w = \mu \left(\frac{\partial u}{\partial r} \right)_w \tag{5}$$

Completing the expression for the analysis is the boundary layer growth rate

$$\delta = (0.37)\ (Z - Z_U)\ [N_{Re}(Z)]^{-1/5} \tag{6}$$

Eliminating $N_{Re}(Z)$ and solving explicitly for $(\partial u/\partial r)_w$, one obtains

$$\left(\frac{\partial u}{\partial r} \right)_w = \frac{(0.0296)}{(0.37)} \frac{\rho \delta}{(Z - Z_U)} (|\dot{S}| + |u|)^2 \tag{7}$$

Using these equations on the data of the type shown on Figures 8 and 9, the results given in Table 1 are obtained. Figure 8 corresponds to the first row and Figure 9 to the second row in the table. In all cases the water flows showed a more rapid movement of eddies toward the centerline than did the polymer flows.

The model used to predict wall shear rates is a steady flow model applied to an unsteady situation. However, the time required for the eddies to travel from the wall to the centerline was of the order of time required for ½ cycle of the sleeve motion. It is also realized that the entire wall did not impose the same stresses on the flow. The model assumes the entire wall to be moving counter to the flow at the sleeve velocity. It tends to underpredict the shear rates at the sleeve wall because it averages the influence of the moving sleeve and the nonmoving tube wall. Use of the conservative velocity difference (Max $|\dot{S}| + |u_{CL}|$) tends to compensate for the underprediction. The model can only be used for obtaining reasonable estimates of wall shear rates and not exact values.

Bruce and Schwarz (*6*) present experimental data on the viscosity and normal stresses for dilute polymer solutions. To obtain estimates for the relationship between these two, their data must be extrapolated. Such an extrapolation yields a value of shear rate equal to 1,000 sec.$^{-1}$ as the shear rate above which elastic effects in a 20 ppm. Separan solution would be observed. At this shear stress the viscosity is only slightly greater than water. Estimates of the wall shear rates in Table 1 fell below the "critical" value of 1,000 sec.$^{-1}$. The highest shear rate created by the moving sleeve in this work was in the ½-in. tube with Reynolds number at 2,000 with the sleeve set at 2-in. amplitude and ½ Hz. At that condition, the estimated shear rate was about 1,000 sec.$^{-1}$, but no other effects were noted that were not present at the lower shear rates. Since a higher viscosity of the polymer solution would lead to a more rapid wake spread for the dilute polymer solution, the observed difference between water and dilute polymer must lie in the structure of the flow field and the relationship between the energy distributed in the random eddies and the periodic motion. Barnard and Sellin (*1*) also measured the rate of spread of a turbulent jet in low concentration solutions (between 0 and 30 ppm.) of polyethylene oxide. The turbulent jet spread rate was about 35% less in the 20 ppm. polyethylene oxide flow than in water. The portions of the wakes laying closest to the tube centerline have the characteristics of a free jet as does the outer region of any turbulent layer.

TABLE 1.

N_{Re}	Frequency, Hz	Diameter, in.	Max. sleeve speed, ips	Amplitude*	Max. shear stress, sec.$^{-1}$
1000	0.25	0.534	1.58	0.3	82
2000	0.25	1.0	1.58	0.28	77
1000	0.50	0.534	3.14	0.6	187
2000	0.25	1.0	3.14	0.56	157
2000	0.50	1.0	6.28	1.12	~350

* Ratio of maximum sleeve velocity to maximum laminar flow velocity.

The failure of viscous effects to accurately predict the behavior of polymer flows in the near field raises a question as to whether demarcation into viscous and elastic effects is adequate. Interaction of the fluid with the disturbance generator occurred at the wall. But the difference noted between polymer and water flows was also seen at the pipe centerline where conditions were much different. The findings here indicate that using wall shear rates to categorize effects as either viscous or elastic is not sufficient.

In the stability literature the disturbance velocity is usually represented as a function periodic in both time and space.

$$u' = u_1' \, e^{i\,[\phi + \omega(t - t_1) + \omega c Z]} \tag{8}$$

Analytical studies assume an infinitesimal disturbance of amplitude u_1' to be created at some time t_1 throughout a given spatial region, and the decay or amplification of the disturbance with time is monitored. The coefficient of time ω is a complex function.

A slightly different approach is necessary in experimental work. In experiments the disturbance is created continuously at some point Z_1, and the spatial history is monitored. The coefficient of distance C must be complex

$$C = C_r + C_i \tag{9}$$

So the experimental disturbance may be represented by

$$u' = u_1' \, e^{-\omega C_i (Z - Z_i)} \, e^{i[\phi + \omega t + C_r (Z - Z_1)]} \tag{10}$$

A positive value of C_i produces a damped disturbance, whereas a negative value of C_i gives an amplified oscillation. C_i is called the "inverse damping rate," and has dimensions of (time/length).

The approach discussed above is generally applied to infinitesimal disturbances, but the same approach can also be used to compare the large amplitude periodic disturbances produced in this study. The choice of u_1' was rather important to the results obtained. Since the periodic disturbance reached a maximum value and always decayed past that point, it was decided that u_1' should be the amplitude of the periodic disturbance at the point of maximum amplitude, Z_1. The damping rate was always positive for $Z > Z_1$.

Following small disturbance stability theory, one may ratio the magnitude of the fluctuating velocity at Z to that at Z_1 to obtain

$$\frac{u'}{u_1'} = e^{-\omega C_i (Z - Z_1)} \tag{11}$$

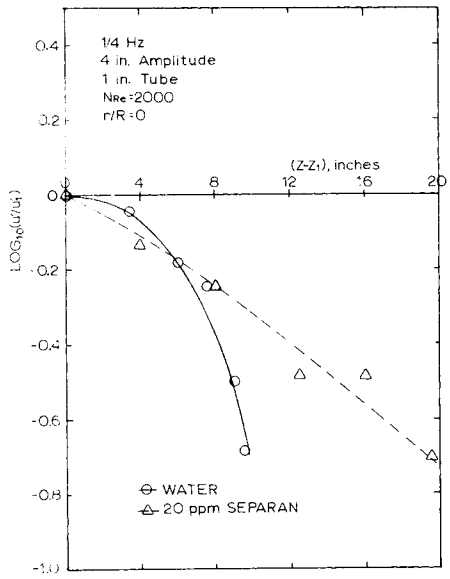

Fig. 13. Log_{10} (u'/u'_1) as a function of distance for water and Separan showing difference in damping rates of the periodic wave.

Comparison of plots of the log u'/u_1' versus Z for the water and dilute polymer solution is then a comparison of the inverse damping rate. A typical plot is shown in Figure 13. All of the data show a more rapid decay of the periodic fluctuations in the water flows.

Since the polymer affects C_i, one might ask of its effect on C_r, the real part of the distance coefficient. C_r is called the inverse wave speed, and like C_i, has dimensions (time/length). C_r can be determined experimentally by measuring the distance required for the periodic fluctuation to go through a 360° cycle. The distance is called the wavelength λ. Then, when $(Z - Z_1) = \lambda$, the spatial phase angle is

$$\omega C_r (Z - Z_1) = \omega C_r \lambda = 2\pi \tag{12}$$

and

$$C_r = \frac{2\pi}{\omega\lambda}$$

Values of C_r have been measured for water and for polymer flows under identical conditions. The phase angles varied linearly with distance. So far as could be determined, no difference existed between the phase angles of polymer and water flows. Thus, under identical flow conditions, C_r was the same for water and polymer flows. The nondimensional wave speed $C_r \overline{U}_{AVE}$ had a value of about 1.05 when the sleeve frequency was ¼ Hz, and dropped to 0.86 when sleeve frequency was set at ½ Hz.

In the intermediate field the eddies had reached the centerline. Alternate laminar and turbulent slugs passed a given point on the centerline. The laminar slugs, with their greater centerline velocity, overtook the turbulent slugs and were destroyed. The distance required for the destruction of the laminar slugs was found to be greater in polymer flows than in water. Explanation of the persistence of the laminar slugs in polymer flows is related to the mean velocities of the laminar and turbulent slugs as well as their structure. The near field accounts for the propagation of the eddies created at the wall to the pipe centerline. In each case the formation step was the same, but by the time the maximum fluctuation is observed at the centerline the situation is quite different in water and dilute polymer solutions. The intermediate field represents the interaction of almost turbulent and laminar slugs for water with a large difference in velocity at the centerline at the interface. Much less difference in velocity was observed for the dilute polymers. Because of the velocity differences in water and polymer flows, the laminar slugs overtake the turbulent slugs at a slower rate in the polymer solutions, thus prevailing longer.

The above discussion is concerned primarily with the interaction of the front of the laminar slugs with the rear of the turbulent slugs. Of course, at the rear of the laminar slugs, there was a tendency to pull away from the turbulent slugs. The flow visualization studies cited earlier determined that the trailing turbulent slugs appeared to stretch out at their leading edges to move into the volume vacated by the laminar slugs. Elastic effects are not important since under the experimental conditions, maximum shear rates at the wall were only near 100 sec.$^{-1}$ and at the turbulent-laminar interface 1 sec.$^{-1}$. It appears that the dilute polymer situation is characteristic of the true decay of the disturbance while in water the interaction of the laminar and turbulent slugs quickly obliterates the periodic character. The true disturbance then behaves the same in each case.

The beginning of the far field is designated at the point at which the laminar slugs completed their encroachment on the turbulent slugs and had been destroyed in the process. Downstream of that point, the original disturbance could only be found by statistical analysis. At the low Reynolds numbers utilized in the detailed experiments, the turbulence was not self-sustaining. Decay of the eddies occurred as the flow moved downstream and the flow returned toward the laminar velocity profile. In the ½-in. tube, the minimum values of the velocity curves do not drop to the value for fully developed turbulent flow. For water in the 1-in. tube, developed turbulent flow velocity was approached. The polymer flows were further removed from full development than were water flows. No appreciable difference in the rate of return of the centerline velocity to the laminar value could be seen in the far field. Based on velocity-time traces and on comparative probability density functions, it is clear that velocity fluctuations were less in the polymer flows indicating fewer high frequency components. The observations of Barnard and Sellin (*1*) and of Gadd (*16*) appear to be consistent with this indication.

Although the far field turbulence was not fully developed, reasonable estimates of the wall shear rates can be made assuming developed turbulent flow. The highest value occurred when $N_{Re} = 2{,}000$ in the ½-in. tube. From Schlichting

$$\left(\frac{\partial u}{\partial r}\right)_w = \frac{(0.3169)}{8}\left(\frac{1}{N_{Re}}\right)^{0.25}\frac{\rho\overline{U}_{AVE}}{\mu} \tag{13}$$

The maximum $(\partial u/\partial r)_w = 125$ sec.$^{-1}$, well below the critical value of 1,000 sec.$^{-1}$ Other investigators such as Wells (*27*) and Meyer (*22*) found elastic and normal stress effects in the form of drag reduction to begin at much higher Reynolds numbers and shear rates. Differences observed in the far field are again due to differences in the structure of the flow.

CONCLUSIONS

In summary, the experimental creation of a disturbance in pipe flows leads to a complex response which must be studied in detail. A thin annular sleeve oscillating at the

wall of a circular pipe creates downstream flow patterns which can be broken into three regions. The first is the near field where the separation wake of the sleeve moves to the tube centerline. Next is the intermediate field where alternate laminar and turbulent slugs are seen to pass a given point. The third is the far field after the laminar slugs are devoured by the turbulent slugs and the flow is turbulent. This turbulence decays at the low Reynolds numbers established in this study. In each region, the water flows and dilute polymer flows exhibited different behavior. In the near field, the wake spreading rate in water was greater than that in the polymer flow. In the intermediate field, the laminar slugs were devoured by turbulent slugs more rapidly in water flow than in polymer flow. Finally, in the far field the turbulence was less well developed in polymer flows than in water flows.

The apparent cause of the anomalies between water and polymer flows was the difference in the random eddy structure in the turbulent portions of the flow created by the backward motion of the sleeve. After the initial interaction of disturbance generator and fluid, the periodic portions of the velocity fluctuations persist longer in the dilute polymer solutions, while random motions do not contain as many high frequency eddies. To explain the behavior on the basis of continuum theories or simple demarcation into behavior caused by either viscous or elastic effects is not sufficient.

The explanation may rely on the concept of a network or partial network of polymer molecules and agglomerations of molecules. In high Reynolds number flows the network can be broken down. But at low Reynolds numbers used in this work, the structured network could be responsible for retardation of flow fluctuations as well as for characteristics of polymer flows sometimes attributed to viscous effects. This is similar to results shown by Ferry (*14*) for much higher frequency studies, and this phenomenon may also occur in dilute polymer solutions at higher frequencies.

The results of this work imply that the transition to turbulence would be delayed in dilute polymer solutions but large amplitude fluctuations at low frequencies can persist in these solutions without leading to turbulence.

ACKNOWLEDGMENTS

The authors are indebted to Mr. Loren Schrenk and Mr. Chen Lin Chang for assisting with the experimental work, and to Capt. John Bacs for some preliminary measurements.

NOTATION

B = amplitude of sleeve movement
C = complex coefficient of distance in disturbance wave function
D = tube diameter
N_{Re} = Reynolds number, $\rho \overline{U}_{AVE} D/\mu$
$N_{Re}(Z)$ = Reynolds number defined by Equation (2)
R = tube radius
r = radial distance from tube centerline
$R(\tau)$ = autocovariance function
S = distance of sleeve movement
$\dot{S}$ = sleeve velocity
t = time
$\overline{U}$ = time-averaged velocity
u = velocity in axial direction, $\overline{U} + u'$
u' = fluctuating velocity
Z = distance between point of laser beam measurement and most forward point of sleeve motion

Greek Letters

δ = boundary layer growth rate
λ = wavelength of periodic velocity fluctuation
μ = fluid viscosity
ρ = fluid density
τ_w = wall shear stress
ϕ = phase angle
ω = sleeve oscillation rate

Subscripts

AVE = averaged over tube cross section
CL = centerline
i = imaginary part of complex function
p = periodic
r = real part of complex function
U = upstream edge of sleeve
w = wall conditions

LITERATURE CITED

1. Barnard, B. J. S., and R. H. J. Sellin, *Nature,* **222,** 1160 (1969).
2. Berman, N. S., *AIChE J.,* **15,** 137 (1969).
3. ———, and E. E. Cooper, Proc. Conf. on Turbulence Measurements in Liquids, Rolla, Mo. (Sept., 1969).
4. Berman, N. S., and V. A. Santos, *AIChE J.,* **15,** 323 (1969).
5. Bhat, W. F., Ph.D. thesis, Univ. of Rochester, N. Y. (1966).
6. Bruce, C., and W. H. Schwarz, *J. Polymer* Sci. A-2, **7,** 909 (1969).
7. Burke, J. P., and N. S. Berman, 69-WA/FE-13 ASME paper (1969).
8. Castro, W. and W. Squire, *Appl. Sci. Res.,* **18,** 81 (1967).
9. Chang, Chen-Lin, M.S. thesis, Arizona St. Univ., Tempe, (1971).
10. Chung, J. S., Univ. of Michigan College of Eng. Tech. Rept. ORA Project 06505 (November 1969).
11. Denn, M. M., and J. Roisman, *AIChE J.,* **15,** 454 (1969).
12. Dodge, D. W., and A. B. Metzner, *AIChE J.,* **5,** 189 (1959).
13. Edwards, R. V., J. C. Angus, M. J. French, and J. W. Dunning, Jr., *J. Appl. Phys.,* **42,** 837 (1971).
14. Ferry, J. D., "Viscoelastic Properties of Polymers," John Wiley, New York (1961).
15. Fox, J. A., M. Lessen anl W. V. Bhat, *Phys. Fluids,* **11,** 1 (1968).
16. Gadd, G. E., *Nature,* **211,** 169 (1966).
17. George, W. D., Ph.D. thesis, Rice Univ., Houston, Texas (1970).
18. Ginn, R. F., and M. M. Denn, *AIChE J.,* **15,** 450 (1969).
19. Goldstein, R. J., R. J. Adrian, and D. K. Kreid, *Ind. Eng. Chem. Fundamentals* **8,** 498 (1969).
20. Hanson, W. A., D. F. Jankowski and N. S. Berman, *Phys. Fluids,* **12,** (1969).
21. Leite, R. J., *J. Fluid Mech.,* **5,** 81 (1959).
22. Meyer, W. A., *AIChE J.,* **12,** 522 (1966).
23. Platten, J., and R. S. Schechter, *Phys. Fluids,* **13,** 832 (1970).
24. Poreh, M., H. Rubin and C. Elata, Faculty of Civil Eng. Publ. No. 126, AD690264 Technion Israel Inst. of Technol. (1969).
25. Schlichting, Hermann, "Boundary Layer Theory," McGraw-Hill, New York (1955).
26. Seyer, F. A. and A. B. Metzner, *AIChE J.,* **15,** 426 (1969).
27. Wells, C. S., *AIAA J.,* **3,** 1800 (1965).
28. White, W. D., and D. M. McEligot, ASME paper 69 WA/FE-20 (1969).

Manuscript received June 30, 1970; revision received September 9, 1971; paper accepted September 10, 1971.